




Article

Thermally expanded vermiculite as a risk-free and general-purpose sorbent for hazardous chemical spillages

Nguyen Duc Cuong¹, Vu Thi Hue² and Yong Shin Kim^{2,3*} 

¹Department of Bionano Engineering, Hanyang University, Ansan 426-791, Republic of Korea; ²Graduate School of Applied Chemistry, Hanyang University, Ansan 426-791, Republic of Korea and ³Department of Chemical and Molecular Engineering, Hanyang University, Ansan 426-791, Republic of Korea

Abstract

Expanded vermiculite with excellent thermal and chemical stability was investigated as a reliable sorbent for hazardous liquid spillages, including those leading to fire and explosion risks. Many expanded samples were prepared by rapid heating using both different temperatures and dissimilar vermiculite dimensions. Their capabilities for hazard clean-up were correlated with the structural characteristics of expanded vermiculite with slit-shaped porosity. When using optimized vermiculite, the moderate sorption capacities of 1.5–3.0 g g⁻¹ were obtained for various hazardous chemicals, including hydrophilic/hydrophobic organic chemicals and strongly acidic/basic solutions. The sorption capacities depended more strongly on physical properties, such as the pore volume of the sorbent and the density of the absorbed liquid, rather than the vermiculite's chemical composition. The void space interconnected by interparticle/intraparticle pores worked as imbibing pathways due to their capillarity, resulting in the rapid, spontaneous sorption of hazardous chemicals. The hazardous chemicals may be removed from a testing vessel via sorption with an efficiency of >94 wt.% for 10 min. These results demonstrate that the expanded vermiculite may be a potential candidate as a reliable general-purpose sorbent for hazardous materials clean-up under harsh conditions.

Keywords: sorption mitigation, expanded vermiculite, hazardous chemicals, sorbent

(Received 30 October 2018; revised 13 March 2019; Accepted Manuscript published online: 22 July 2019; Associate Editor: Lawrence Warr)

Hazardous chemicals are utilized widely nowadays for various industrial applications. Chemical spills occur during the production, storage and transportation of hazardous substances. These may pose a severe threat to the public and the environment. The risk of hazardous liquids has been reduced by various techniques, including dispersion (Kujawinski *et al.*, 2011), *in situ* burning (Fritz, 2003), sorption (Melvold & Gibson, 1988; Chabot *et al.*, 2014) and bioremediation (Singh *et al.*, 2012). Most of these methods produce secondary chemical pollutants. However, sorption may clean up these hazards without serious side effects. The use of inert sorbents is an efficient and promising approach for the mitigation of hazardous spillages.

A great number of sorbents have been investigated for cleaning up spills of petroleum products using natural minerals such as zeolites, clays and diatomaceous materials (Bastani *et al.*, 2006; Medeiros *et al.*, 2009; Bandura *et al.*, 2017), natural organics such as wood fibres, feathers and wool (Radetic *et al.*, 2008; Rajaković-Ognjanović *et al.*, 2008), synthetic polymers (Zhu *et al.*, 2011; Yati *et al.*, 2016) and macroporous carbon materials (Bi *et al.*, 2012; Wu *et al.*, 2014; Ge *et al.*, 2017; Ren *et al.*, 2017). Although advanced carbon materials exhibited a greater sorption capacity for oil and organic chemicals than other sorbents, there are still several technical and practical issues relating to their application. Most carbon sorbents are unsatisfactory at

sorption of aqueous chemicals due to the highly hydrophobic nature of carbon. Their macroporous structures are destroyed by the fires and explosions that often accompany chemical accidents, and they become inactive under high-temperature conditions. The problem of burning is more serious when using organic-based sorbents such as natural organics and synthetic polymers. Furthermore, cost-effective sorbents are required in large quantities to mitigate large-scale chemical accidents. Some advanced sorbents based on carbon macrostructures (Bi *et al.*, 2012; Wu *et al.*, 2014; Ren *et al.*, 2017) and synthetic polymer composites (Zhu *et al.*, 2011) with excellent sorption capabilities are available in sponge or mat forms. Nevertheless, expensive equipment and long processing times hamper the large-scale production of these advanced sorbents. It is a challenge to develop affordable, environmentally harmless sorbents with acceptable sorption capacities and excellent thermal/chemical stabilities.

Vermiculite is a natural 2:1 phyllosilicate formed by the hydrothermal alteration of mica. Vermiculite flakes are exfoliated or expanded to produce concertina-shaped granules by thermal shock at ~1000°C (El Mouzdahir *et al.*, 2009; Marcos *et al.*, 2009; Marcos & Rodríguez, 2010). The exfoliation relies on an impulsive build-up of the steam produced by evaporating interlayer water within the mosaic-like multiphase lamellar structures (Hillier *et al.*, 2013). Expanded vermiculite has remarkable properties: it is lightweight and has low thermal conductivity, it is chemically inert, has a high melting point and good sorption ability due to its capillary pore structure and active silicate surface (Valášková & Martynková, 2012; Rashad, 2016). These properties are required in order for ideal sorption of liquid hazards to work

*E-mail: yongshin@hanyang.ac.kr

Cite this article: Cuong ND, Hue VT, Kim YS (2019). Thermally expanded vermiculite as a risk-free and general-purpose sorbent for hazardous chemical spillages. *Clay Minerals* 54, 235–243. <https://doi.org/10.1180/clm.2019.34>

effectively under harsh conditions. While the absorption characteristics of expanded vermiculite have been investigated extensively for pollutant removal from aqueous solutions (Duman *et al.*, 2015; Marcos & Rodríguez, 2016; Bourliva *et al.*, 2018), there has been very limited study of the absorption mitigation of hazardous chemical spillages (Melvold & Gibson, 1988). Recently, ultrathin layered silicates were incorporated into graphene oxide beads to produce a fire-retardant sorbent for cleaning up hazardous chemicals (Bao *et al.*, 2016). The hybrid graphene oxide beads were synthesized using a long coagulation process followed by freeze-drying. The graphene oxide ingredient was calcined at $>550^{\circ}\text{C}$. Moreover, the involvement of coagulation agents may generate toxic, volatile by-products through chemical reactions with the absorbed hazards. Therefore, a cheap and inert sorbent is still desired for the mitigation of large-scale spillages of hazardous chemicals.

The main objective of this work is to study the relationship between the structural parameters (particle dimensions and textural properties) and sorption performance of chemically inert, thermally stable vermiculite for evaluating its potential as a general-purpose sorbent for land-based spillages of hazardous chemicals. To the best of our knowledge, the dependence of sorbent performance on structural features has not been studied in detail for expanded vermiculite, although the effects of the sorbent's dimensions and textural properties have been investigated in synthetic zeolite produced from fly ash (Bandura *et al.*, 2015, 2016). Here, commercially available Palabora vermiculite was further classified according to its particle size and thickness to prepare more homogeneous samples. The textural features of expanded vermiculite obtained at different heating temperatures were characterized for the size-selected samples using material analysis techniques. The sorption behaviour was investigated in terms of the sorption capacity, removal efficiency and imbibition rate to verify the importance of textural control in the sorption process. Furthermore, the expanded vermiculite with an optimized structure was confirmed to be a universal sorbent for various hazardous liquids (hydrophilic/hydrophobic organic chemicals and strongly acidic/basic aqueous solutions). The affordable vermiculite sorbent exhibited both a fast imbibition speed and an excellent removal efficiency through the optimization of particle dimensions and pore-size distribution.

Materials and methods

Materials and chemicals

Three different grades (medium, superfine and micro) of raw vermiculite (Palabora, South Africa) were obtained from Shingsung Mineral (South Korea). Ethanol, toluene, benzene, methyl ethyl ketone, furfuryl alcohol, acrylic acid, ethyl acetate, *m*-cresol and ammonium hydroxide (28 wt.%) were purchased from Daejung Chemicals & Metals (South Korea). Methanol and allyl chloride were obtained from Junsei Chemical (Tokyo, Japan). 2-Nitrotoluene and nitric acid (30 wt.%) were purchased from Acros Organics (India) and Merck Millipore (Germany), respectively. All chemicals were of reagent grade and used without further purification.

Preparation of expanded vermiculite

The commercially available vermiculites had a broad particle-size distribution (micro = 0.25–0.71 mm; superfine = 0.35–1.00 mm; medium 1.40–4.00 mm). To improve dimensional homogeneity,

the vermiculite was classified according to its planar size using a sieving machine and was then further categorized by thickness through a weight-based separation process. The dimensions of the separated samples are summarized in Table 1. The planar size and thickness were determined as average values obtained by measuring 50 vermiculite flakes. Thermal expansion experiments were performed by using a tube furnace at temperatures of 400°C , 700°C and 1000°C . To generate a thermal shock, a crucible containing vermiculite was loaded quickly into the furnace stabilized at a pre-set temperature and removed after 5 min. The expanded vermiculite was stored in a desiccating cabinet and dried at 150°C in a vacuum oven for 1 h before use. The density of the sample was measured using a balance (GX-200, A&D, Japan) equipped with a density-determination kit (GX-13, A&D). The expansion ratio was calculated using Eq. (1).

$$\text{Expansion ratio} = \frac{D_0}{D} \quad (1)$$

where D_0 and D are the densities of crude and expanded vermiculite, respectively. The expansion ratio was determined by averaging the values obtained from three measurements.

Material characterization

The microstructure and atomic composition were determined by scanning electron microscopy (SEM; Hitachi S-4800), using a SEM device equipped with an energy-dispersive X-ray spectrometer (EDS). To probe crystalline structures, X-ray diffraction (XRD) traces were obtained by using an X-ray diffractometer (Rigaku D/MAX-2500) with $\text{Cu-K}\alpha_1$ ($\lambda = 1.54056 \text{ \AA}$) radiation at 40 kV, 100 mA and a scanning step of $0.02^{\circ}2\theta$. Mercury porosimetry (AutoPore IV 9500, Micromeritics, USA) was used to characterize the specific surface area, pore volume and pore-size distribution.

Evaluation of sorption performance

The sorption was characterized in terms of the sorption capacity, removal efficiency and imbibition rate of liquid chemicals. To determine the sorption quantity, 1.0 g vermiculite samples were placed in a meshed stainless steel cell with square openings of 0.5 mm. The cell was fully immersed in a vessel containing a test solvent and then shaken at a rate of 60 rpm for 30 min, permitting the liquid chemical to penetrate into the pores of the vermiculite. Then it was lifted out from the container and held until the interval between successive drops was >10 s. Subsequently, the meshed cell was placed on absorbing paper to further remove excess solvent. The vermiculite absorbent was discharged from the cell and spread over a polyethylene terephthalate film to eliminate the excess liquid that is present in the voids among the particles. Shortly afterwards, the weight of the sample absorbed (M_{abs}) was recorded using a balance, and the dry mass (M_{dry}) was quantified after drying in a vacuum oven at 150°C for 1 h. Finally, the sorption capacity, defined by the relative weight of absorbed liquid to sorbent, was calculated using Eq. (2).

$$\text{Sorption capacity} = \frac{M_{\text{abs}} - M_{\text{dry}}}{M_{\text{dry}}} \quad (2)$$

Three measurements were performed to obtain the average sorption capacity and its variation.

Table 1. Summary of the average dimensions of raw vermiculite used in this work.

	Sample ID	Planar size ^a (mm)	Thickness ^a (μm)
Series #1	S1	0.84 ± 0.14	150 ± 50
	S2	2.40 ± 0.40	500 ± 180
	S3	4.20 ± 0.70	560 ± 200
Series #2	SS1	0.93 ± 0.16	220 ± 70
	SS2	1.20 ± 0.20	270 ± 120
	SS3	1.60 ± 0.30	360 ± 120
	SS4	2.50 ± 0.50	240 ± 110
	SS5	4.50 ± 0.50	270 ± 120
	SS6	6.00 ± 1.00	240 ± 150

^aThe mean and standard deviation values were obtained from measuring 50 samples.

The removal efficiency was quantified using the percentage weight of removed liquid substance with respect to the initial amount. For this purpose, 10 g of vermiculite and 20 g of liquid chemical were used. The liquid was poured into a cylindrical reservoir and its initial weight (M_0) was measured precisely using a balance. A stainless steel mesh container with a 0.5 mm gap was filled with a sample and was then introduced into the chemical-containing vessel for 10 min. The sorbent container was lifted out and held until the interval between successive drops was >10 s. The weight of the remaining solvent (M) was recorded. The removal efficiency was calculated using Eq. (3).

$$\text{Removal efficiency} = \frac{M_0 - M}{M_0} \times 100 \quad (3)$$

The efficiency depends on the dimensions of both the liquid container and the sample cell. In this work, the outside diameter of the cell was ~10 mm smaller than the inside hole of the reservoir (diameter ~55 mm).

The imbibition rate was evaluated from the capillary rise speed of water in a vertical configuration along a glass tube (diameter = 8 mm) packed with expanded vermiculite (Kirdponpattara *et al.*, 2013). To achieve a densely packed column, 0.5 g of vermiculite was placed manually in a glass tube blocked with a Parafilm® layer at the bottom, and the sample-containing tube was dropped 100 times from a height of ~20 cm. This procedure was repeated three more times for the packing of a 2 g sample. After detaching the Parafilm, the vermiculite-packed column was mounted vertically on a scaffold connected to a balance (GX-200, A&D). A suspended water vessel was raised manually using a jack until the bottom of the column was just in contact with the water. The uptake mass of spontaneously imbibed water was recorded as a function of time.

Results and discussion

Thermal expansion behaviours

A photograph of vermiculite samples thermally treated at 400°C, 700°C and 1000°C is shown in Fig. 1a, together with an untreated sample. They were prepared using the same amount of sample S1 with a planar size of 0.84 ± 0.14 mm and a thickness of 150 ± 50 μm. A distinct volume increase at >700°C was noted in terms of the expansion or exfoliation of raw vermiculite, as has been previously reported for vermiculite with a layered structure (El Mouzdahir *et al.*, 2009; Marcos & Rodríguez, 2010). To quantify the degree of expansion, the expansion ratio was determined for various samples with dissimilar dimensions at different

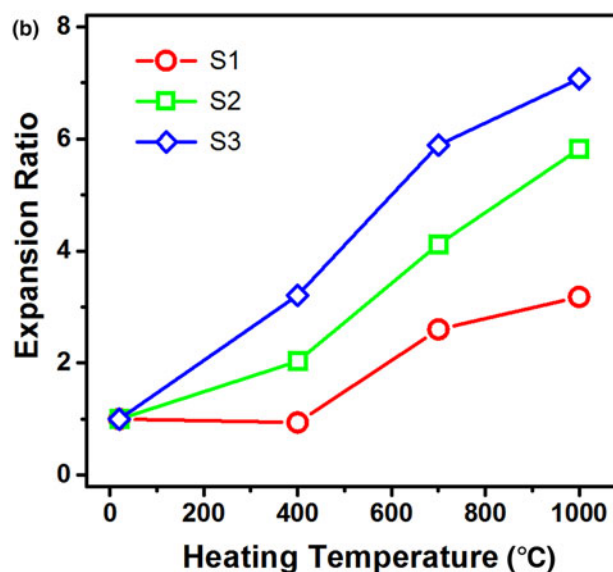
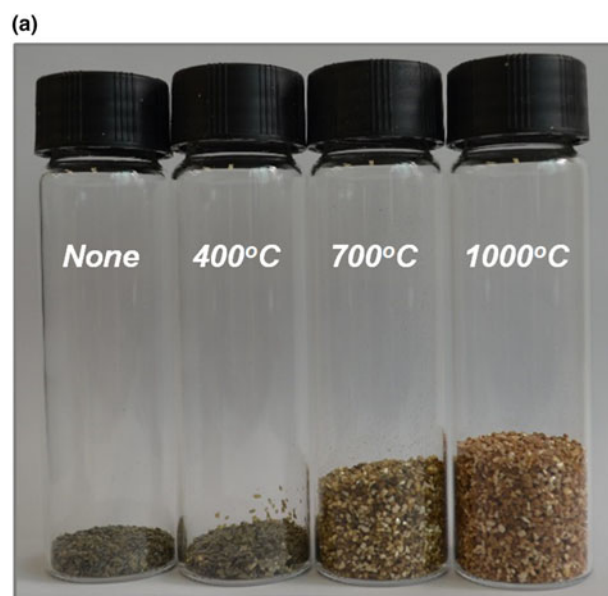


Fig. 1. (a) Photograph of thermally treated vermiculite at the designated temperatures using sample S1. (b) Curves of the expansion ratios as a function of the heating temperature for the three samples S1–S3 with different dimensions. Each expansion ratio was determined by averaging the values obtained from three measurements.

treatment temperatures. Figure 1b shows the temperature dependence of the expansion ratio for vermiculite with three different dimensions (samples S1–S3 in Table 1), exhibiting greater expansion both for larger samples and at higher temperatures. The highest value was 7.1 for sample S3 heated at 1000°C with an average planar size of 4.2 mm. The temperature and size dependences of the expansion ratio may be explained by the exfoliation mechanism proposed by Hillier *et al.* (2013): the expansion results from a build-up of steam pressure formed by the release of interlayer water in mosaic-like intergrown vermiculite during rapid heating. The evaporation of interlayer water was confirmed by XRD, as described below. Because larger vermiculite has more mosaic-layer structures acting as a maze for the escaping gaseous

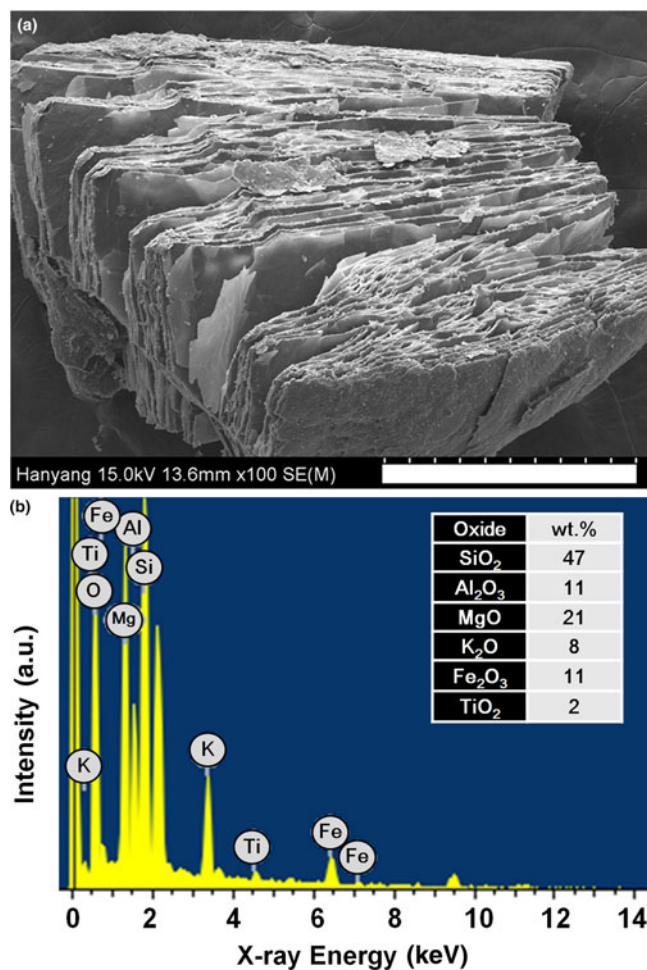


Fig. 2. (a) SEM image and (b) EDS spectrum of vermiculite expanded at 1000°C using sample S1. The scale bar in (a) corresponds to 500 μm .

molecules, it may expand intensively due to the effective retention of the steam generated. The thermal expansion of vermiculite takes place when the build-up of pressure exceeds the bonding forces between the layers.

Material characterization

Material properties of expanded vermiculite were examined to understand the exfoliation process in detail. Figure 2a shows a typical SEM image of one vermiculite particle (sample S1) expanded at 1000°C, illustrating a delaminated structure with different gaps. The delaminated morphology with slit-shaped porosity clearly indicates the intensive volume expansion in terms of thickness without fragmentation via thermal shock. The degree of expansion was significantly heterogeneous from particle to particle. The chemical composition of the vermiculite used was probed by EDS analysis (Fig. 2b). The composition obtained is summarized in the inset table in Fig. 2b, which agrees with previously reported results (Marcos *et al.*, 2009; Marcos & Rodríguez, 2010). The high K₂O content at 8 wt.% suggests that the dominant phase of Palabora vermiculite corresponds to the interstratification of mica and vermiculite layers (hydrobiotite) rather than pure vermiculite. The hydrobiotite had been reported to provide

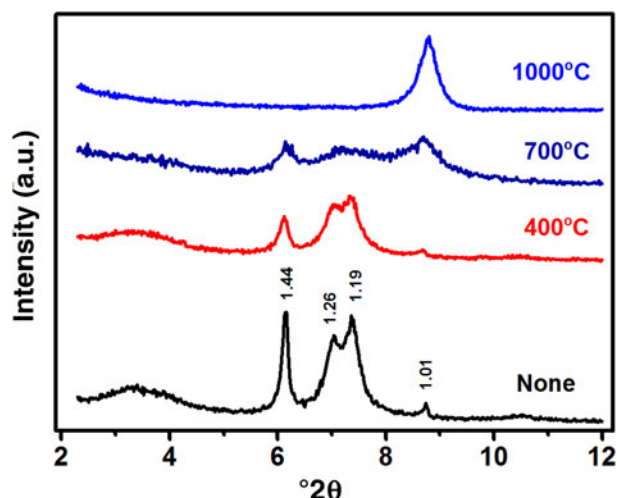


Fig. 3. Powder XRD traces of vermiculite expanded at different temperatures of 400°C, 700°C and 1000°C together with the crude form. Sample S1 was used for these experiments.

a greater propensity for exfoliation than true vermiculite (Hillier *et al.*, 2013). The high degree of expansion may be attributed to the interstratified structure that is responsive to the extensive formation of the mosaic-like intergrown layer.

The amount of interlayer water was monitored by means of the first-order basal spacing of layered vermiculite. Powder XRD traces of crude and expanded vermiculite (sample S1) in a low 2θ angle region are shown in Fig. 3. The raw material exhibits three intense reflections at 6.13°, 7.00° and 7.43° and a weak peak at 8.73°, corresponding to the interplanar distances of 1.44, 1.26, 1.19 and 1.01 nm, respectively. They had previously been assigned to different water-layer hydration states (WLHS): 2-WLHS for 1.44 nm, 2/1-WLHS for 1.26 nm, 1-WLHS for 1.19 nm and 1/0-WLHS for 1.01 nm (Suzuki *et al.*, 1987; Udoudo *et al.*, 2015). Therefore, the crude sample may be interpreted as showing the coexistence of highly hydrated states, while the 1000°C sample is dominated by the less hydrated 1/0-WLHS. The dehydrated peak is significantly enhanced at >700°C, which is in good agreement with the temperature dependence of the expansion ratio (Fig. 1b). These observations support the expansion mechanism based on the thermal dehydration of interlayer water.

The size distribution of slit holes in expanded vermiculite is a key factor in many useful applications, such as thermal insulation, water retention and the absorption of soundwaves. The pore-size distributions characterized by Hg porosimetry are shown in Fig. 4. Sample S1 (planar size = 0.84 mm) heated at 400°C exhibits one dominant peak centred at $\sim 250 \mu\text{m}$, while sample S1 heated at 1000°C displays a bimodal distribution with an additional maximum at 1.9 μm . Because the 400°C sample displayed negligible exfoliation, a pore diameter of >100 μm was assigned to artificial pores caused by the void spaces between particles (Giesche, 2006). The interparticle pore diameters are frequently associated with the packing conditions of the particles. On the other hand, the 1.9 μm peak at 1000°C can be interpreted as the void gap between delaminated layers in expanded vermiculite. A featureless population in the middle region of 5–100 μm is also regarded as being a result of the slit holes with conical openings, indicating a broad macroporous size distribution within expanded vermiculite. A pore-size distribution of sample S2 with a planar size of 2.4 mm was characterized in order to examine the effect of vermiculite particle size. The larger

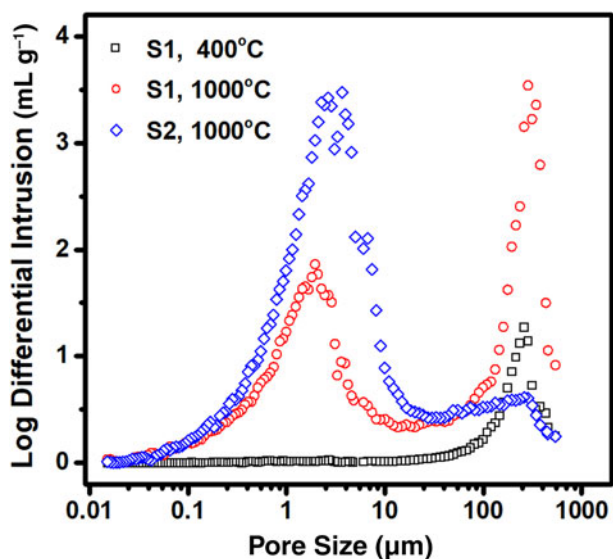


Fig. 4. Distributions of the pore size probed by Hg porosimetry for different samples and temperatures: sample S1 expanded at 400°C, sample S1 expanded at 1000°C and sample S2 expanded at 1000°C.

vermiculite particles exhibited a stronger peak at the larger pore size of $\sim 3 \mu\text{m}$. The pore volumes and areas obtained for various samples by the Hg porosimeter are summarized in Table 2. Extensive separation among the silicate layers is possible when large vermiculite flakes expand at high temperatures.

Liquid-absorbing characteristics of expanded vermiculite

Fundamental absorption characteristics were quantified in terms of the sorption capacity, removal efficiency and imbibition rate for non-toxic ethanol. Figure 5a shows the variation curves of the sorption capacity as a function of heating temperature for three samples with different particle dimensions (samples S1–S3). The sorption capacity increased steadily for all samples when the temperature increased, as observed in the expansion ratio (Fig. 1b). However, the temperature dependence of the sorption capacity was quantitatively different from that of the expansion ratio for the samples with a different size. For example, the sorption capacities of the samples prepared at 1000°C are similar at $\sim 1.9 \text{ g g}^{-1}$, while the expansion ratio of sample S3 is 2.2 times larger than that of sample S1. Because during absorption the liquid is taken inside the spaces of the expanded vermiculite, the sorption capacity can be more directly correlated with the pore volume determined by Hg porosimetry. Figure 5b presents the variation in sorption capacity with respect to pore volume, which displays a good proportional relationship for the smallest sample S1. This result implies that the sorption capacity depends heavily on the total pore volume of a sample, including intraparticle and interparticle voids. Nevertheless, the dependence of the sorption capacity on pore volume became weak for samples of different sizes, suggesting the involvement of additional factors in the sorption process.

In order to further clarify the dimension-dependent change, the expansion ratio and the sorption capacity at 1000°C were determined for vermiculite samples SS1–SS6, having different planar sizes in the range of 0.9–6 mm and similar thicknesses of $\sim 270 \mu\text{m}$. Figure 6 shows the variations in the expansion ratio

Table 2. Summary of the pore volumes and pore areas determined by Hg porosimetry.

Sample ID	Temperature (°C)	Pore volume ($\text{cm}^3 \text{g}^{-1}$)	Pore area ($\text{m}^2 \text{g}^{-1}$)
S1	400	0.59	0.14
	700	2.44	4.36
	1000	3.65	13.00
S2	1000	4.20	15.80
S3	1000	4.81	18.00

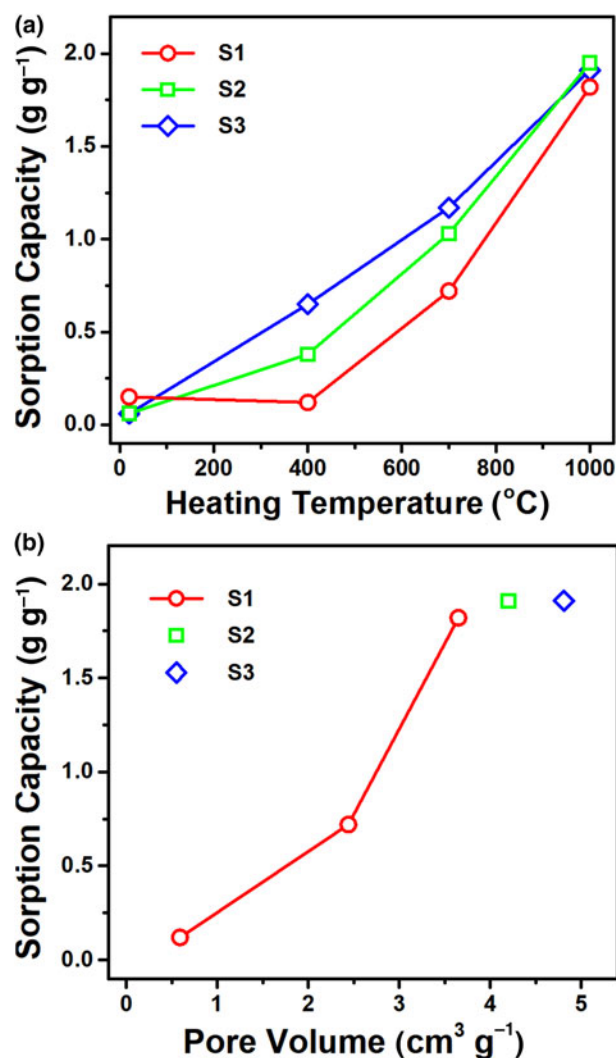


Fig. 5. (a) Plots of the sorption capacities as a function of heating temperature for samples S1–S3. (b) Variation of the sorption capacities with respect to pore volume. Three measurements were performed to determine average values of the sorption capacities.

and sorption capacity with respect to planar size, demonstrating a weak size dependence of the sorption capacity despite the steady increase in the expansion ratio. A plausible explanation for this may be the different efficiencies of liquid uptake according to the particle size. Interparticle spaces $>1 \text{ mm}$ not spontaneously infilled by ethanol were observed in large samples (planar size $>4 \text{ mm}$), which implies a low uptake efficiency into very large pores. The thermal shock produces numerous slit pores with a triangle-like inward shape. When the planar particle size was large, ethanol would be partially infilled into the triangular

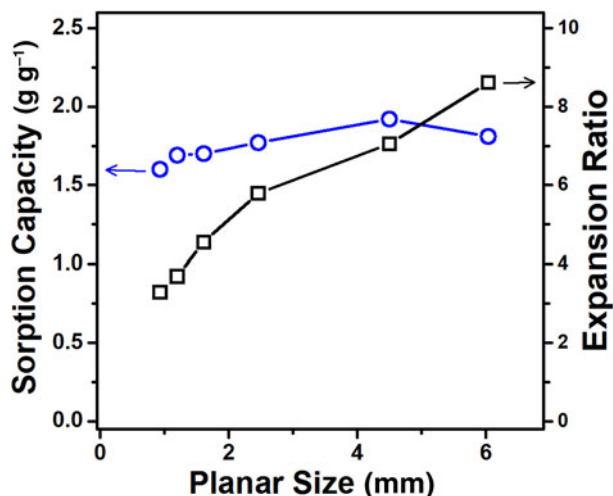


Fig. 6. Variations of the sorption capacities and the expansion ratios with respect to the planar size of vermiculite. Three measurements were performed to determine average values of the sorption capacities and the expansion ratios.

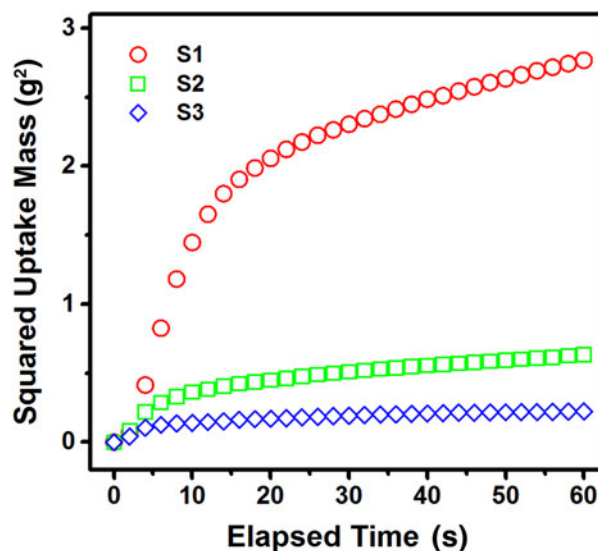


Fig. 8. Time-profiled curves of the squared mass of imbibed water along the glass tubes packed with vermiculite expanded at 1000°C using samples S1-S3. Each curve was obtained from three replicated experiments.

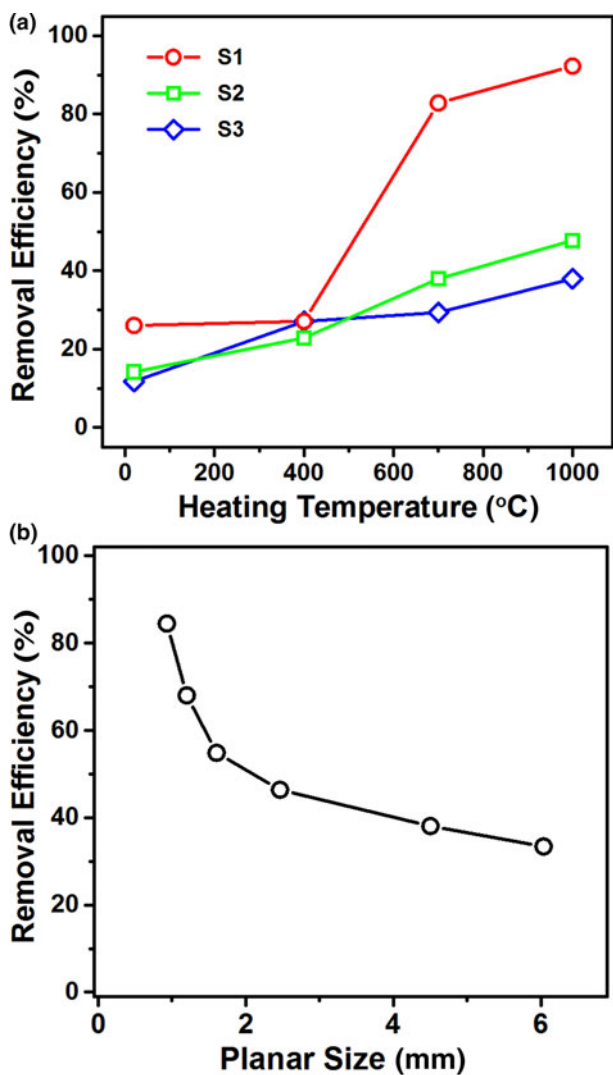


Fig. 7. (a) Plots of removal efficiencies as a function of the heating temperature for samples S1-S3. (b) Curve of the removal efficiency with respect to the planar size of expanded vermiculite.

pores and mainly retained at the corners of these pores due to the surface tension of the liquid (Mason & Morrow, 1991). Therefore, the dimensional features of intraparticle/interparticle pores are considered to play a key role in controlling the sorption behaviour.

The removal efficiency was examined in order to evaluate the applicability of expanded vermiculite to the fast, spontaneous mitigation of hazardous chemicals via sorption. Figure 7a shows the variations in removal efficiency of ethanol as a function of the heating temperature, demonstrating a maximum value for the smallest sample S1 expanded at 1000°C. These variations indicate that the removal efficiency is heavily dependent on the particle size together with the heating temperature. The enhancement of removal efficiency at higher temperatures may be explained by the additional generation of intraparticle pores, resulting in larger pore volumes. At 1000°C, the removal efficiencies were 92.3 wt.% for sample S1, 47.8 wt.% for sample S2 and 38.0 wt.% for sample S3. The thermally untreated vermiculite has considerable uptake efficiency in the range of 12–26 wt.%. These results suggest the involvement of the void spaces between vermiculite particles for liquid adsorption. The excellent removal efficiency of small vermiculite particles suggests the occurrence of capillarity-driven sorption into interparticle/intraparticle pores. In order to examine the size dependence of sorption in more detail, the removal efficiency was also evaluated for samples SS1–SS6 expanded at 1000°C. Figure 7b shows a plot of removal efficiency vs. planar size, which exhibits a reciprocal-like curve. The size-dependent variation might be correlated with the capillary pressure (P_c):

$$P_c = \frac{2\gamma\cos\theta}{r_{\text{eff}}} \quad (4)$$

where r_{eff} is the effective radius of the void channels in expanded vermiculite, γ is the surface tension and θ is the contact angle. Because tiny vermiculite particles develop intraparticle/interparticle pores with small radii, a strong capillary force may result in a high removal efficiency. The size-dependent variation is at odds with the trend observed in the sorption capacity, which may be attributed to

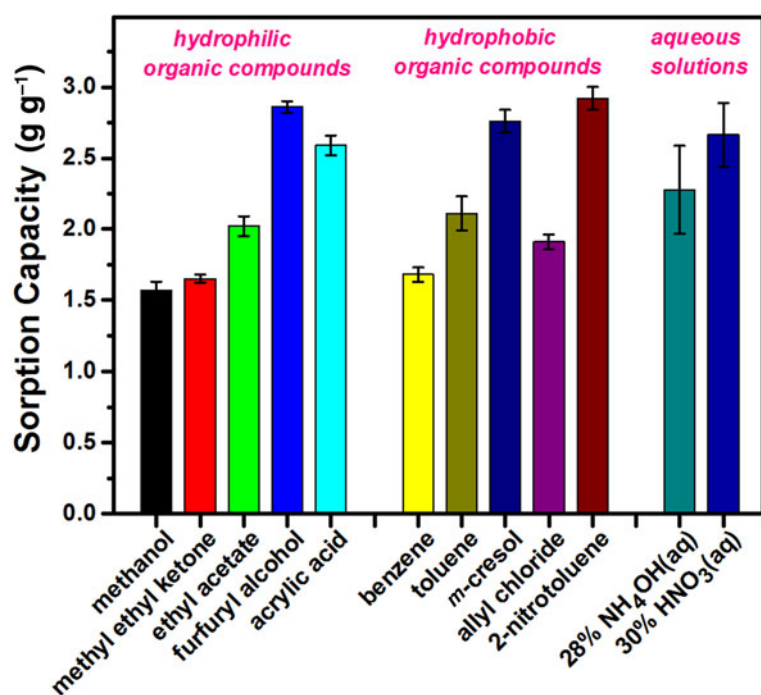


Fig. 9. Bar graph of the sorption capacities for various hazardous chemicals. The vertical error bars indicate variations of the sorption capacity obtained from triplicate measurements.

the difference in the key controlling factors: pore volume for the sorption capacity and pore size for the removal efficiency.

In order to better understand the size dependence of removal efficiency, the wicking dynamics of water were studied using a glass column packed with expanded vermiculite. Figure 8 shows the time-dependent variations of a squared water uptake mass for samples S1–S3, which display a linear increase in squared mass only during an initial period of ~10 s. Afterwards, the wicking rate was greatly reduced and the uptake mass approached a saturated value within several minutes. The smallest sample S1 exhibited faster imbibition than samples S2 and S3, indicating a strong dependence of the uptake rate on the sample dimension. The saturated water uptake weights after 15 min were 2.6 g for the small sample S1, 1.1 g for the medium sample S2 and 0.6 g for the large sample S3. A stabilized uptake mass (m_s) is possible under balanced conditions between the capillary pressure (P_c) and the hydrostatic pressure ($P_h = \rho gh$). The stabilized m_s value can be expressed by the relationship $m = \rho Ah\epsilon$ as:

$$m_s = \frac{2A\epsilon\gamma\cos\theta}{gr_{\text{eff}}} \quad (5)$$

where A is the cross-sectional area of the glass tube, ϵ is the porosity of the packed expanded vermiculite, ρ is the liquid density and g is the gravitational acceleration. In separated experiments, the porosity was quantified to show little variation (<5 vol.%) for the three different columns. Assuming that the density and the contact angle are constant for the same type of liquid and sorbent, the greater uptake mass of sample S1 is predominantly ascribed to the narrower effective radius (r_{eff}) for water flow. Furthermore, the wicking kinetics into porous expanded vermiculite is described by the modified Lucas–Washburn equation (Kirdponpattara *et al.*, 2013):

$$m^2 = \frac{C\rho^2\gamma\cos\theta}{\eta} t \quad \text{with } C = \frac{r_{\text{eff}}A^2\epsilon^2}{2} \quad (6)$$

where m is the weight of an imbibed liquid, C is the geometric factor, η is the viscosity of the liquid and t is the elapsed time after the contact with water. The Lucas–Washburn theory may explain the linear change of the squared uptake mass in the first short interval. The deviation from the model equation for a long period of elapsed time may be interpreted as being due to the wicking kinetics, which in turn are strongly affected by parameters such as a broad size distribution of the voids (Kirdponpattara *et al.*, 2013), a delaminated slit-like pore shape (Nishi *et al.*, 2002) and heterogeneity in the packing density (Dang-Vu & Hupka, 2005). The consecutive packing processes created heterogeneity in the column density, along with loose connections at the top and large voids near the tube wall due to a wall effect (Mehta & Hawley, 1969). As a result, the pore-size distribution formed by expanded vermiculite is a critical factor in regulating the liquid removal process based on spontaneous wicking.

Absorptive mitigation testing of hazardous chemicals

The sorption capacity and the removal efficiency were determined for 12 hazardous liquid chemicals using sample S1 expanded at 1000°C. The liquids tested are representative hazardous substances classified as hydrophilic organic compounds, hydrophobic organic compounds and acidic/basic aqueous solutions. The sorption capacities obtained vary in the range 1.5–3.0 g g⁻¹ (Fig. 9). These values are greater than the sorption capacities of 0.8–1.2 g g⁻¹ that were previously reported for soybean, engine and diesel oils when using expanded vermiculite (Medeiros *et al.*, 2009). However, because the sorption capacity also relies on the physical properties of the sorbate, such as viscosity and density (Bandura *et al.*, 2015; Ge *et al.*, 2017), these factors should be considered for a reasonable comparison. Our sorption capacities do not reveal any strong dependence on the different types of substances, indicating a weak relationship between the sorption capacity and the physicochemical properties of the hazardous liquid, such as hydrophilicity and molecular structure. This result indicates that expanded vermiculite may be utilized to mitigate

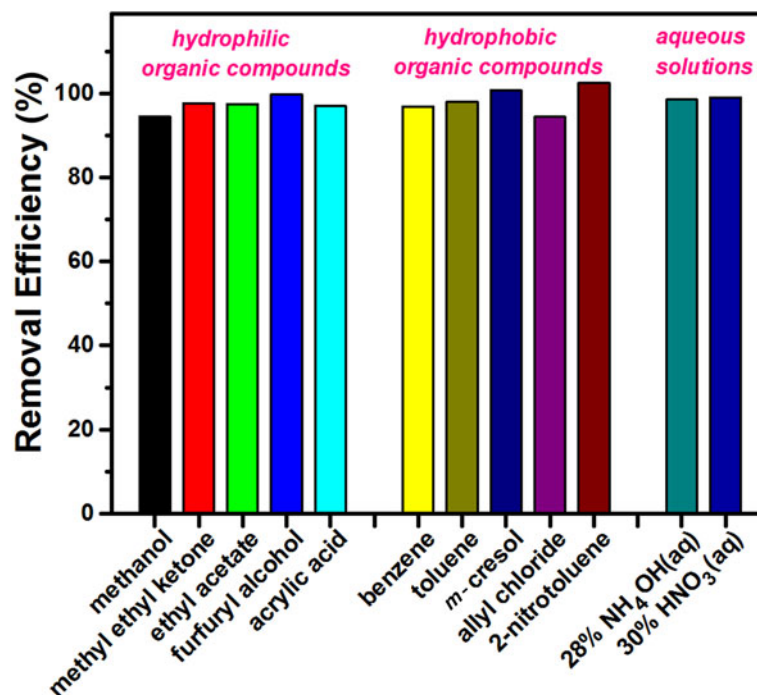


Fig. 10. Bar graph of the removal efficiencies for various hazardous chemicals.

various kinds of hazardous spillages without serious degradation or side effects. The sorption capacity was correlated significantly with the density of the hazardous chemical. Compounds with a density of $>1 \text{ g cm}^{-3}$ (furfuryl alcohol, acrylic acid, *m*-cresol, 2-nitrotoluene and 30 wt.% HNO₃(aq)) have higher sorption capacities, while the light methanol, methyl ethyl ketone and benzene have lower sorption capacities. This density-dependent increase in the sorption capacity was previously reported in the sorption of diesel and engine oils using zeolite sorbents (Bandura *et al.*, 2015). When the sorption capacity was expressed by a hazard volume per unit weight of sorbent, the converted value was in the range of 2.0–2.6 cm³ g⁻¹. This is smaller than the pore volume of 3.65 cm³ g⁻¹ measured by Hg porosimetry, suggesting an incomplete filling of liquid chemicals into the interparticle/intraparticle pores, probably due to the very large pore size, the existence of trapped air and/or the incompatible interface property between vermiculite and the adsorbate. Consequently, a pore volume of acceptable size is regarded as a crucial parameter for determining the sorption capacity. In order to increase the sorption capacity of vermiculite, the formation of macroporous vermiculite structures via H₂O₂-based chemical expansion will be assessed in the future.

The removal efficiency was also quantified for the same harmful chemicals to evaluate their comparative spontaneously wicking ability. Figure 10 shows a bar graph of removal efficiencies grouped into the three hazard categories. All of them exhibit excellent removal efficiency, exceeding 94 wt.%. There is no distinct dependence on the types of absorbed chemicals, which supports the notion that the imbibition-based removal process is predominantly affected by physical features such as the pore-size distribution, as mentioned above, rather than chemical interactions between the liquid molecule and the sorbent.

Conclusions

A universal sorbent is needed to mitigate large-scale hazard spillages under harsh conditions (including high temperature and strongly

acidic and alkaline conditions) without environmental risk or leading to secondary pollution. To achieve this goal, the sorbent must be cheap, thermally stable, chemically inert, highly porous and mechanically durable. Even though some polymer-based materials and macroporous carbons have been reported to have a very high sorption capacity, there is no sorbent that satisfies all of the requirements perfectly. Palabora vermiculite was tested here and evaluated as a risk-free, general-purpose sorbent that is appropriate for most hazardous chemicals because it is naturally abundant, easy to prepare, chemically inert and thermally stable. The sorption capacity and the removal efficiency were optimized by controlling the dimensions and macroporous structures of the expanded vermiculite. The macroporous structure dependence was explained by capillarity-driven imbibition. These sorption performances were insensitive to the chemical properties of hazardous chemicals, demonstrating the capability of expanded vermiculite as a general-purpose sorbent, based on testing 12 types of liquids classified into different chemical classes. Furthermore, there exists an additional opportunity to improve the sorbent performances through improved expansion and/or surface modification of vermiculite. The advanced vermiculite-based clay sorbent could be used to mitigate petroleum oils spilled on seawater and impermeable land.

Acknowledgements. This research was supported both by the Korea Ministry of Environment (MOE) as the Environmental Technology Development Program of the ‘Chemical Accident Prevention Technology Development Project’ and by the Basic Science Research Program through the National Research Foundation of Korea (NRF) funded by the Ministry of Education (2018R1D1A1B07041567).

References

- Bao C., Bi S., Zhang H., Zhao J., Wang P., Yue C.Y. & Yang J. (2016) Graphene oxide beads for fast clean-up of hazardous chemicals. *Journal of Materials Chemistry A*, **4**, 9437–9446.
- Bastani D., Safekordi A.A., Alihosseini A. & Taghikhani V. (2006) Study of oil sorption by expanded perlite at 298.15K. *Separation & Purification Technology*, **52**, 295–300.

- Bandura L., Franus M., Józefaciuk G. & Franus W. (2015) Synthetic zeolites from fly ash as effective mineral sorbents for land-based petroleum spills cleanup. *Fuel*, **147**, 100–107.
- Bandura L., Panek R., Rotko M. & Franus W. (2016) Synthetic zeolites from fly ash for an effective trapping of BTX in gas stream. *Microporous and Mesoporous Materials*, **223**, 1–9.
- Bandura L., Wozuk A., Kolodynska D. & Fronus W. (2017) Application of mineral sorbents for removal of petroleum substances: a review. *Minerals*, **7**, 37–61.
- Bourliva A., Sikalidis A.K., Papadoulou L., Betsiou M., Michailis K., Sikalidis C., & Filippidis A. (2018) Removal of Cu²⁺ and Ni²⁺ ions from aqueous solutions by adsorption onto natural palygorskite and vermiculite. *Clay Minerals*, **53**, 1–15.
- Bi H., Xie X., Yin K., Zhou Y., Wan S., He L., Xu F., Banhart F., Sun L. & Ruoff R.S. (2012) Spongy graphene as a highly efficient and recyclable sorbent for oils and organic solvents. *Advanced Functional Materials*, **22**, 4421–4425.
- Chabot V., Higgins D., Yu A., Xiao X., Chen Z. & Zhang J. (2014) A review of graphene and graphene oxide sponge: material synthesis and applications to energy and the environment. *Energy & Environmental Science*, **7**, 1564–1596.
- Dang-Vu T. & Hupka J. (2005) Characterization of porous materials by capillary rise method. *Physicochemical Problem of Mineral Processing*, **39**, 47–75.
- Duman O., Tunç S. & Polat T.G. (2015) Determination of adsorptive properties of expanded vermiculite for the removal of C. I. Basic Red 9 from aqueous solution: kinetic, isotherm and thermodynamic studies. *Applied Clay Science*, **109–110**, 22–32.
- El Mouzdahir Y., Elmchaouri A., Mahboub R., Gil A. & Korili S.A. (2009) Synthesis of nano-layered vermiculite of low density by thermal treatment. *Powder Technology*, **189**, 2–5.
- Fritz D.E. (2003) *In situ* burning of spilled oil in freshwater inland regions of the United States. *Spill Science & Technology Bulletin*, **8**, 331–335.
- Ge J., Shi L.-A., Wang Y.-C., Zhao H.-Y., Yao H.-B., Zhu Y.-B., Zhang Y., Zhu H.-W., Wu H.-A. & Yu S.-H. (2017) Joule-heated graphene-wrapped sponge enables fast clean-up of viscous crude-oil spill. *Nature Nanotechnology*, **12**, 434–440.
- Giesche H. (2006) Mercury porosimetry: a general (practical) overview. *Particle & Particle Systems Characterization*, **23**, 9–19.
- Hillier S., Marwa E.M.M. & Rice C.M. (2013) On the mechanism of exfoliation of 'vermiculite'. *Clay Minerals*, **48**, 563–582.
- Kirdponpattara S., Phisalaphong M. & Newby B.Z. (2013) Applicability of Washburn capillary rise for determining contact angles of powders/porous materials. *Journal of Colloid & Interface Science*, **397**, 169–176.
- Kujawinski E.B., Kido Soule M.C., Valentine D.L., Boysen A.K., Longnecker K. & Redmond M.C. (2011) Fate of dispersants associated with the Deepwater Horizon oil spill. *Environmental Science & Technology*, **45**, 1298–1306.
- Marcos C. & Rodríguez I. (2010) Expansion behaviour of commercial vermiculites at 1000°C. *Applied Clay Science*, **48**, 492–498.
- Marcos C. & Rodríguez I. (2016) Thermoexfoliated commercial vermiculites for Ni²⁺ removal. *Applied Clay Science*, **132–133**, 685–693.
- Marcos C., Arango Y.C. & Rodríguez I. (2009) X-ray diffraction studies of the thermal behaviour of commercial vermiculites. *Applied Clay Science*, **42**, 368–378.
- Mason G. & Morrow N.R. (1991) Capillary behavior of a perfectly wetting liquid in irregular triangular tubes. *Journal of Colloid Interface Science*, **141**, 262–274.
- Medeiros M.A., Sansiviero M.T.C., Araújo M.H. & Lago R.M. (2009) Modification of vermiculite by polymerization and carbonization of glycerol to produce highly efficient materials for oil removal. *Applied Clay Science*, **45**, 213–219.
- Mehta D. & Hawley M.C. (1969) Wall effect in packed columns. *Industrial & Engineering Chemistry Process Design and Development*, **8**, 280–282.
- Melvold R.W. & Gibson S.C. (1988) A guidance manual for selection and use of sorbents for liquid hazardous substance releases. *Journal of Hazardous Materials*, **17**, 329–335.
- Nishi Y., Iwashita N., Sawada Y. & Inagaki M. (2002) Sorption kinetics of heavy oil into porous carbons. *Water Research*, **36**, 5029–5036.
- Radetic M., Ilic V., Radojevic D., Miladinovic R., Jovic D. & Jovancic P. (2008) Efficiency of recycled wool-based nonwoven material for the removal of oils from water. *Chemosphere*, **70**, 525–530.
- Rajaković-Ognjanović V., Aleksić G. & Rajaković Lj. (2008) Governing factors for motor oil removal from water with different sorption materials. *Journal of Hazardous Materials*, **154**, 558–563.
- Rashad A.M. (2016) Vermiculite as a construction material – a short guide for civil engineer. *Construction & Building Materials*, **125**, 53–62.
- Ren R.-P., Li W. & Lv Y.-K. (2017) A robust, superhydrophobic graphene aerogel as a recyclable sorbent for oils and organic solvents at various temperatures. *Journal of Colloid Interface Science*, **500**, 63–68.
- Singh B., Bhattacharya A., Channashettar V.A., Jeyaseelan C.P., Gupta S., Sarma P.M., Mandal A.K. & Lal B. (2012) Biodegradation of oil spill by petroleum refineries using consortia of novel bacterial strains. *Bulletin of Environmental Contamination & Toxicology*, **89**, 257–262.
- Suzuki M., Wada N., Hines D.R. & Whittingham M.S. (1987) Hydration states and phase transitions in vermiculite intercalation compounds. *Physical Review B*, **36**, 2844–2851.
- Udoudo O., Folorunso O., Dodds C., Kingman S. & Ure A. (2015) Understanding the performance of a pilot vermiculite exfoliation system through process mineralogy. *Minerals Engineering*, **82**, 84–91.
- Valášková M. & Martynková G.S. (2012) Vermiculite: structural properties and examples of the use. Pp. 209–238 in: *Clay Minerals in Nature – Their Characterization, Modification and Application* (M. Valášková & G.S. Martynkova, editors). InTech, London, UK.
- Wu Z.-Y., Li C., Liang H.-W., Zhang Y.-N., Wang X., Chen J.-F. & Yu S.-H. (2014) Carbon nanofiber aerogels for emergent cleanup of oil spillage and chemical leakage under harsh conditions. *Scientific Reports*, **4**, 4079.
- Yati I., Aydin G.O. & Sonmez H.B. (2016) Cross-linked poly(tetrahydrofuran) as promising sorbent for organic solvent/oil spill. *Journal of Hazardous Materials*, **309**, 210–218.
- Zhu H., Qiu S., Jiang W., Wu D. & Zhang C. (2011) Evaluation of electrospun polyvinyl chloride/polystyrene fibers as sorbent materials for oil spill cleanup. *Environmental Science & Technology*, **45**, 4527–4531.